

STORM TIME RING CURRENT - ATMOSPHERE INTERACTIONS: OBSERVATIONS AND MODELLING

V. K. Jordanova⁽¹⁾, C. G. Mouikis⁽¹⁾, L. M. Kistler⁽¹⁾, H. Matsui⁽¹⁾, P. Puhl-Quinn⁽¹⁾ and Y. Khotyaintsev⁽²⁾

⁽¹⁾University of New Hampshire, Space Science Center, Durham, NH 03824, USA, Email: vania.jordanova@unh.edu

⁽²⁾Swedish Institute of Space Physics, Uppsala, Sweden, Email: yuri.khotyaintsev@irfu.se

ABSTRACT

During periods of increased solar and geomagnetic activity charged particles are injected from the magnetotail, and being transported sunward and accelerated, build the storm time ring current. The currents induced simultaneously in the ionosphere and on the Earth's surface disturb telecommunications, navigation satellites, and power grids. Understanding ring current dynamics is, therefore, crucial for predicting the Earth-related impacts of the solar wind plasma flow. In this paper we investigate the ring current-atmosphere interactions during the October 2001 geomagnetic storm using our kinetic drift-loss model employing a) Volland-Stern, or b) Weimer large-scale convection electric field models. Calculated distribution functions are compared with multi-point observations of energetic particles from the Cluster Ion Spectrometry (CIS) instrument, while the large-scale convection electric field models are compared with Cluster Electron Drift Instrument (EDI) and Electric Field and Wave (EFW) data. Both convection models showed good overall agreement with CIS in-situ data, however, Volland-Stern model underestimated the fluxes within the stagnation dip at low L . Strong EMIC waves were excited by the anisotropic ring current ion distributions and caused enhanced proton precipitation into the atmosphere near Dst minima.

1. INTRODUCTION

The terrestrial ring current has an important role in the transport of energy from the Sun through the inner magnetosphere into the subauroral ionosphere. A large fraction of the solar wind energy extracted by the magnetosphere is stored in the storm time ring current as it builds up during the main phase of the storm. This energy is subsequently released during the recovery phase of the storm causing plasmaspheric electron and ion heating, energetic neutral and ion precipitation, and the excitation of stable auroral red arcs. The anisotropic ring current populations generate plasma waves that could subsequently accelerate and/or scatter radiation belt particles. Understanding ring current dynamics, i.e., energetic particle transport, acceleration, and loss is therefore a central issue in geomagnetic storm studies. Recent modelling, theory, and observations indicate that the ring current is a highly dynamic region and a

complete understanding of the mechanisms involved in ring current formation and decay requires study on a global scale. New advances in ring current modelling using multiple satellite observations are presented in this paper.

2. OBSERVATIONS

2.1 Interplanetary Data from ACE

We investigate ring current dynamics during the large storm of 21 October 2001. This storm had a rapid main phase reaching minimum $Dst = -187$ nT and maximum $Kp = 8^-$ at approximately 22 UT (Fig. 1). The analysis of

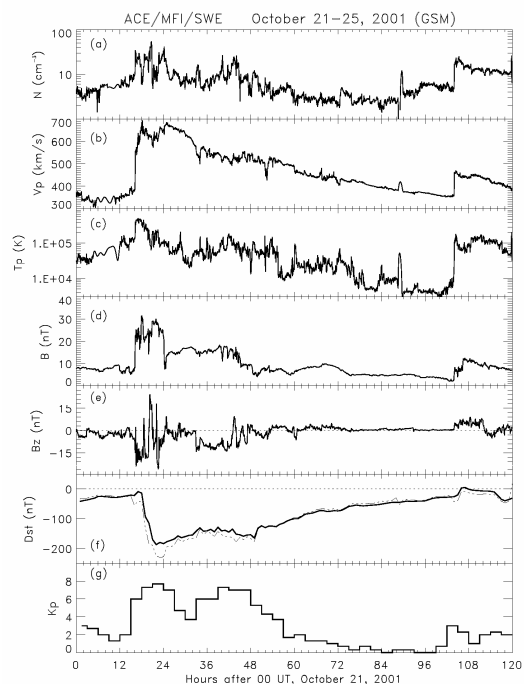


Fig. 1. Interplanetary observations from the MFI and SWEPAM instruments on ACE (a) proton density, (b) solar wind bulk speed, (c) proton temperature, (d) magnetic field strength, (e) the B_z (GSM) component of the magnetic field. (f) The measured Dst (solid) and magnetopause currents corrected Dst (dashed-dotted) indices, and (g) the planetary Kp index.

ACE interplanetary magnetic field (IMF) and plasma data [1, 2] indicates that it was triggered by the sheath of a magnetic cloud at about 16 UT when the associated interplanetary shock reached Earth. The IMF B_z component was fluctuating within the sheath region and decreased to about -20 nT, while the solar wind speed increased to ~ 700 km/s. The IMF B_z reached a second negative excursion of about -15 nT within the magnetic cloud at ~ 9 UT on 22 October, followed by a second maximum $Kp=7^+$ and minimum $Dst=-165$ nT at ~ 1 UT on 23 October, and a slow storm recovery lasting for several days.

2.2 Magnetospheric Data from CLUSTER

Data from an inner magnetosphere pass of the Cluster Ion Spectrometry (CIS) experiment on Cluster are shown in Fig. 2. CIS measures the 3-dimensional distribution functions of the major ring current ion species, H^+ , He^+ , and O^+ over the energy per charge range 20-40000 eV/e. It is a combination of a top-hat electrostatic analyzer followed by post-acceleration by 15 kV and a time-of-flight measurement. It sweeps through the full energy range 32 times per spin, so that the full distribution is obtained once per spin period [3]. The CIS data shown in Fig. 2 are from ~ 20 -24 UT on 21 October 2001, when Cluster perigee was near the magnetic equatorial plane in the dayside local time sector.

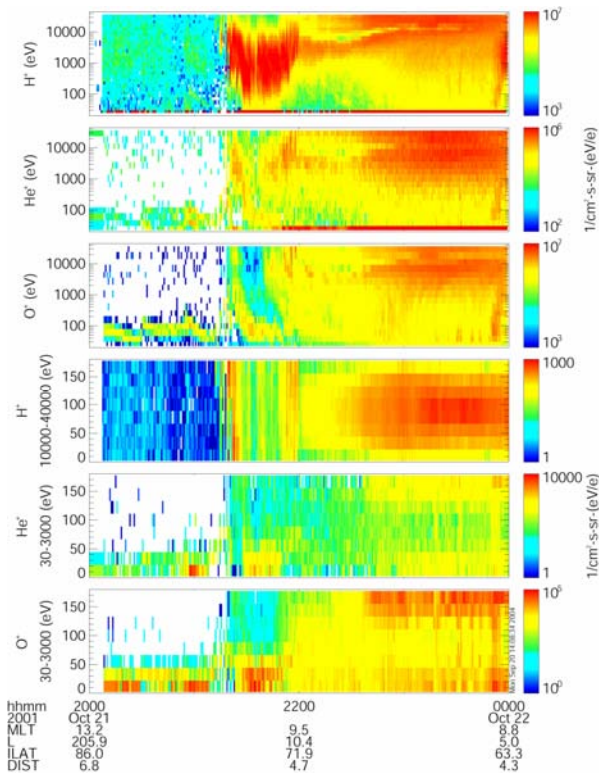


Fig. 2. Energy and pitch angle spectra for H^+ , He^+ , and O^+ as the Cluster spacecraft 4 goes toward perigee (ephemeris data are tabulated at the bottom).

The energy spectra clearly show the deep stagnation minimum at about 10 keV in all species due to the slow velocity. Low energy heavy ion ionospheric outflows are observed near 21 UT. In the inner magnetosphere, at high energies H^+ distribution peaks at 90° pitch angle, while at low energy O^+ and He^+ have field aligned distributions.

The Electron Drift Instrument (EDI) on Cluster measures electric fields on the basis of injection of weak beams of 1-keV electrons and their detection after one or more gyrations in the ambient magnetic field \mathbf{B} . The EDI technique is highly sensitive to the relatively weak convection electric fields seen in the inner magnetosphere. EDI measures both components of the convection electric field (in the plane perpendicular to \mathbf{B}) for arbitrary orientations of \mathbf{E} and \mathbf{B} with respect to the spacecraft spin axis [4]. The Electric Field and Wave (EFW) experiment on Cluster is designed to measure quasi-static electric fields of amplitudes up to 700 mV/m with high amplitude and time resolution down to 0.1 ms. The sensor system of the instrument consists of four orthogonal cable booms; the potential difference between two opposite spherical sensors on orthogonal booms provides the average electric fields in two directions [5].

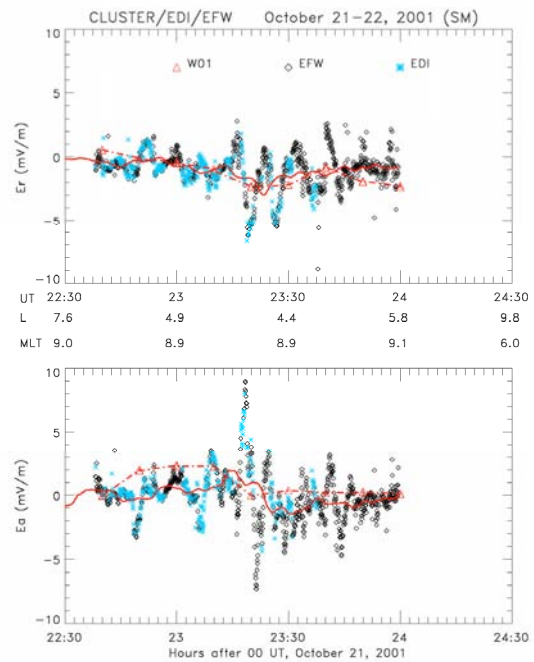


Fig. 3. Data from the EDI (stars) and the EFW (diamonds) investigation on Cluster spacecraft 1 compared to Weimer model (triangles connected with dash-dot line). The solid line indicates 10-min averages of the data.

As noted above there are two instruments that measure the electric field on Cluster. Because both instruments have some data gaps, it is worthwhile to merge the two

complementary data sets. The merged electric fields from EDI and EFW at in-situ spacecraft locations during the October 2001 storm are shown in Fig. 3. The fields are mapped to the magnetic equator in the solar magnetospheric (SM) coordinate system for each 4 s using the Tsyganenko [6] magnetic field model. We assume the magnetic field lines are equipotentials. As for the input parameters of the Tsyganenko model, the interplanetary magnetic field (IMF) and solar wind data are taken from ACE. SYM-H index is taken from the World Data Center at Kyoto University. The effect of the gradient \mathbf{B} drift of 1 keV electron beams is subtracted from the original EDI data by using the Tsyganenko model during the mapping procedure. We have also calculated data with 10 min resolutions by taking running averages in order to highlight DC components and ULF (Pc 5) wave components. The averaged radial component of the merged EDI and EFW electric fields (solid line) agrees well with the one calculated from Weimer [7] model (dashed-dotted line), however, there are significant differences between the two azimuthal components. These differences indicate that the particles do not flow outward at ~ 23 UT as the model predicted. Another feature is that there is a large ULF wave component. These are the toroidal oscillations that may be related to the acceleration of radiation belt electrons [8].

3. MODEL RESULTS

We simulated the storm time injection and trapping of energetic ions during the 21 October 2001 storm employing our kinetic ring current-atmosphere interaction model (RAM) [9, 10]. The model solves the bounce-averaged kinetic equation for the distribution function in the equatorial plane from 2 to 6.5 R_E radial distances and all magnetic local times (MLT). H^+ , O^+ , and He^+ particles with kinetic energy from ~ 150 eV to ~ 500 keV, and equatorial pitch angle from 0° to 90° are considered. The loss terms include charge exchange with geocoronal hydrogen, Coulomb collisions with thermal plasma, pitch angle scattering by electromagnetic ion cyclotron (EMIC) waves, convective loss through the dayside magnetopause, and precipitation of ring current particles at low altitude with a timescale of half a bounce period. The loss cone implies a 200 km altitude of the dense atmosphere.

We compared the ring current evolution obtained with two inner magnetospheric convection models: (a) the 3 hour averaged Kp -dependent Volland-Stern model [11, 12, 13] and (b) the Weimer [7] model where we input interplanetary data at 10 min resolution. To make a smooth transition between the different electric potential distributions, we interpolated linearly. The corotation potential was kept the same in both approaches and the magnetic field of the Earth was approximated as a dipole magnetic field model. As initial conditions we

used the quiet time statistical data set obtained from the CHEM spectrometer on the AMPTE/CCE spacecraft [14] and the empirical quiet time radiation belt model AP8-MAX [15]. The nightside boundary conditions were updated during the storm period according to ion flux measurements from the MPA [16] and SOPA [17] instruments on the geosynchronous LANL satellites.

Distribution functions of H^+ and O^+ ions calculated in the prenoon sector (MLT=9) during the main phase of the storm are compared with observations from the CIS instrument (squares) in Fig. 4. There are no large differences between the distributions calculated using the Volland-Stern (dashed-dotted line) or the Weimer (solid line) models at large L shells and both models reproduce well the data. At $L \leq 4.5$, however, Volland-Stern model significantly underestimates the H^+ and O^+ distributions within the stagnation dip.

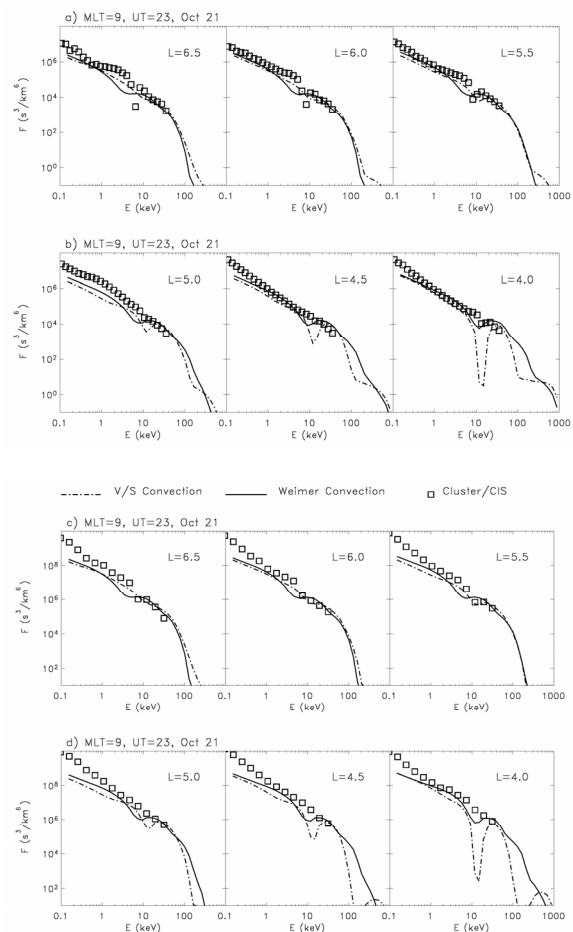


Fig. 4. Comparison of H^+ (a and b) and O^+ (c and d) distribution functions calculated using Volland-Stern (dashed-dotted) or Weimer (solid) model with Cluster/CIS data (squares) at 23 UT on 21 October 2001 at different L shells and MLT=9.

Similar results were obtained by [10, 18] when modelled distributions were compared with Polar/HYDRA and Equator-S/ESIC data. It was found

that ions with small azimuthal velocity drifted at smaller distances from Earth in a Volland-Stern model and thus underwent larger losses, leading to wider dips in the distribution functions. This effect was more pronounced at lower L shells, where particles encountered higher geocoronal and plasmaspheric densities.

The wave gain of He^+ band EMIC waves excited by the unstable ring current ion distributions, calculated with our model during the October 2001 storm, is shown in Fig. 5a. In order to treat the process of wave-particle interactions self-consistently, we calculate the equatorial growth rate of EMIC waves from the hot plasma dispersion relation, which is solved simultaneously with the kinetic equation. Strong EMIC waves were excited when the ring current intensified during the main phase and near Dst minima at hours ~ 24 and 48. The unstable regions were primarily located in the postnoon sector and along the plasmapause. Scattering of ring current H^+ ions into the loss cone by resonant interactions with these plasma waves resulted in more than 10% reduction of the ring current energy near Dst minima [19]. Although charge exchange losses were the largest collisional losses during this storm, ion precipitation losses became comparable to charge exchange losses near the peak of the storm, while Coulomb collisions losses remained about two orders of magnitude smaller.

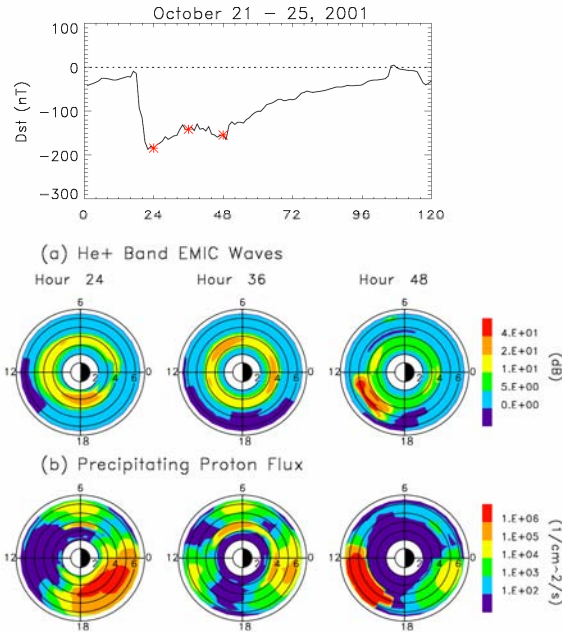


Fig. 5. (a) Wave gain of He^+ band EMIC waves, and (b) precipitating 20-100 keV proton fluxes calculated with our kinetic model as a function of radial distance in the equatorial plane and MLT at several hours after 0 UT, 21 October 2001, indicated with stars on the Dst plot.

Interactions of ring current ions with EMIC waves will scatter resonant particles into the loss cone and cause ion precipitation into the atmosphere. To calculate this

scattering effect on the distribution function and the resulting ion precipitation with our model, we use quasi-linear theory with diffusion coefficients updated simultaneously according to the EMIC wave gain as the storm evolves. Global images of precipitating proton fluxes integrated over 20-100 keV energy range are shown in Fig. 5b. The proton precipitation maximizes in the postnoon to midnight local time sector when plasma wave scattering is included (near hours 24 and 48). This indicates that pitch angle scattering by EMIC waves is a viable mechanism for particle precipitation into the atmosphere and generation of subauroral arcs. The feedback from the wave-induced diffusive changes in the proton distribution on the EMIC wave excitation causes the unstable wave regions to disappear with time as the proton distribution becomes isotropic.

4. CONCLUSIONS

The ring current is a key element of geomagnetic storms and an indicator of the flow of mass and energy through the near-Earth magnetosphere. We simulated ring current-atmosphere interactions during the large storm of 21-25 October, 2001, with our RAM model [10]. We compared results from this global kinetic model driven either by a) Volland-Stern, or b) Weimer convection electric field models and found:

- Weimer model reproduced very well the radial component of the merged Cluster EDI and EFW electric fields, however, significant differences were seen between the modeled and measured azimuthal components.
- The observed CLUSTER/CIS H^+ and O^+ distributions compared well with both models at large L shells. At low L the Volland-Stern model underestimated the fluxes within the stagnation dip, while Weimer model showed good agreement with in-situ CIS data.
- Intense EMIC waves were generated during the main and recovery phases; this caused a significant enhancement of the ion precipitation predicted with the model. Scattering by the EMIC waves reduced by about 10% the total ring current energy.

Future extensions of this work will consider constructing an equatorial convection electric field model of the inner magnetosphere based on merged EDI and EFW data sets. This convection model will be further implemented into the RAM, and the predictive capabilities of RAM will be assessed by comparing its results to in-situ storm time data. Ring current morphology, ion composition, and loss mechanisms during various storm phases will be investigated.

Acknowledgments

This work is supported in part by NASA under grants NAG5-13512 and NNG05GG50G, and NSF under grant ATM-0309585. Thanks are due to M. Thomsen and G. Reeves for supplying us with LANL data, and to D. McComas and N. Ness for ACE data made publicly available on the CDAWeb. The *Dst* index is taken from the World Data Center at Kyoto University, Japan.

References

1. Smith C. W., L'Heureux J., Ness N. F., Acuna M. H., Burlaga L. F. and Scheifele J., The ACE magnetic fields experiment, *Space Sci. Rev.*, 86, 613 - 632, 1998.
2. McComas D. J., Bame S. J., Barker P., Feldman W. C., Phillips J. L., Riley P. and Griffee J. W., Solar wind electron proton alpha monitor (SWEPAM) for the advanced composition explorer, *Space Sci. Rev.*, 86, 563 - 612, 1998.
3. Rème H., et al. The Cluster Ion Spectrometry Experiment, *Space Sci. Rev.*, 79, 303, 1997.
4. Paschmann G., et al. The Electron Drift Instrument for Cluster, *Space Sci. Rev.*, 79, 233, 1997.
5. Gustafsson G., et al. The Electric Field and Wave Experiment for the Cluster Mission, *Space Sci. Rev.*, 79, 137, 1997.
6. Tsyganenko N. A., A model of the near magnetosphere with a dawn-dusk asymmetry 2. Parameterization and fitting to observations, *J. Geophys. Res.*, 107, 1176, doi:10.1029/2001JA000220, 2002.
7. Weimer D. R., An improved model of ionospheric electric potentials including substorm perturbations and application to the Geospace Environment Modeling November 24, 1996, event, *J. Geophys. Res.*, 106, 407, 2001.
8. Elkington S. R., Hudson M. K. and Chan A. A., Acceleration of relativistic electrons via drift-resonant interaction with toroidal-mode Pc-5 ULF oscillations, *Geophys. Res. Lett.*, 26, 3273, 10.1029/1999GL003659, 1999.
9. Jordanova V. K., Kozyra J. U., Nagy A. F. and Khazanov G. V., Kinetic model of the ring current-atmosphere interactions, *J. Geophys. Res.*, 102, 14279, 1997.
10. Jordanova V. K., Kistler L. M., Farrugia C. J. and Torbert R. B., Effects of inner magnetospheric convection on ring current dynamics: March 10-12, 1998, *J. Geophys. Res.*, 106, 29705-29720, 2001.
11. Volland H., A semiempirical model of large-scale magnetospheric electric fields, *J. Geophys. Res.*, 78, 171, 1973.
12. Stern D. P., The motion of a proton in the equatorial magnetosphere, *J. Geophys. Res.*, 80, 595, 1975.
13. Maynard N. C. and Chen A. J., Isolated cold plasma regions: Observations and their relation to possible production mechanisms, *J. Geophys. Res.*, 80, 1009, 1975.
14. Kistler L. M., Ipavich F. M., Hamilton D. C., Gloeckler G., Wilken B., Kremser G. and Stuedemann W., Energy spectra of the major ion species in the ring current during geomagnetic storms, *J. Geophys. Res.*, 94, 3579, 1989.
15. Vette J. I., The NASA/National Space Science Data Center Trapped Radiation Environment Model Program (1964-1991), *NSSDC/WDC-A-RS 91-29*, 1991.
16. McComas D. J., et al., Magnetospheric plasma analyzer: Initial three-spacecraft observations from geosynchronous orbit, *J. Geophys. Res.*, 98, 13453, 1993.
17. Belian R. D., Gisler G. R., Cayton T. and Christensen R., High-Z energetic particles at geosynchronous orbit during the great solar proton event series of October 1989, *J. Geophys. Res.*, 97, 16897, 1992.
18. Kistler L. M., et al., Testing electric field models using ring current ion energy spectra from the Equator-S ion composition (ESIC) instrument, *Ann. Geophys.*, 17, 1611, 1999.
19. Jordanova V. K., Sources, transport, and losses of energetic particles during geomagnetic storms, in *The Inner Magnetosphere: Physics and Modeling*, ed. by T. I. Pulkkinen, N. A. Tsyganenko, and R. H. W. Friedel, AGU, Washington, D. C., p. 9, 2005.